NILU
TEKNISK NOTAT NR: 6/81
REFERENCE: 01080
DATE: MAI 1981

ON HORIZONTAL WIND FIELD ESTIMATION BASED ON A FEW MEASUREMENT STATIONS IN WINTER FLOW OVER OSLO

BY

KARL J. EIDSVIK

NORWEGIAN INSTITUTE FOR AIR RESEARCH
P.O. BOX 130, N-2001 LILLESTRØM
NORWAY

ISBN 82-7247-244-9

SUMMARY

Hourly wind data from 8 measurement stations in Oslo during a winter season are analyzed for spatial structure. It appears that a homogeneous and isotropic version of Gandin's optimal prediction theory adequately explains actual prediction errors in the area spanned by the predictor stations.

The maximum statistical prediction accuracy is estimated to be approximately equal to the prediction accuracy for Grønskei's physical flow model.

A heat island effect over Oslo is verified by an objectively estimated horizontal convergence.

LIST OF CONTENTS

ON HORIZONTAL WIND FIELD ESTIMATION BASED ON A FEW MEASUREMENT STATIONS IN WINTER FLOW OVER OSLO

1 INTRODUCTION

A motivation for this study is that actual atmospheric transport and wind parameters are important for air pollution computations (compare Goodin et al, 1980 and Eidsvik, 1980, 1981). Estimation errors for wind will therefore introduce errors in air pollution estimation. Opinions about the typical magnitudes of such errors differ widely, so that every quantification should be of interest.

Optimal estimation of stochastic vectorial fields, with field dimension higher than one, is of interest to many sciences, albeit a difficult one (Granger, 1965; Katayama, 1980). In meteorology, Gandin (1963) advanced a local approach for scalar variables when the stochastic structure, measurement setup and measurement errors are known. The same framework seems to have been independently developed in geology under the name of "Krieging" (Olea 1975). It is considerably simpler than Sasaki's (1970) global objective techniques.

The Gandin theory is extended to vectorial variables in Appendix A. It is used to estimate roughly, the maximum prediction accuracy of the horizontal wind field over Oslo for various measurement station networks. Statistical predictions are compared with Grønskei's (1973) physical flow prediction method outlined in Appendix B. Since the winds were weak during the measurement period, the signal to noice ratio is small and the results should be considered as tentative only.

2 WINTER FLOW OVER OSLO

2.1 Data

During the period 1 Dec. 1970 to 28 Feb 1971 measurements of hourly mean wind were done at three stations in Oslo (Grønskei et al., 1973). Data from Meteorological Institute stations, recording 10 min averages each second hour, were also available. For the purpose of this study, wind estimates at non-observing hours were extrapolated from the last observation. This constitutes 5 stations with hourly observations of wind. Their locations are shown in Figure 1. In addition, there were 3 stations with hourly data of poorer quality during ca 2 months of operation. Data from two of these are used to verify the prediction based on the first five. The station locations were selected so that the wind measurements should be representative for the general flow over the area. For the purpose of this study, this is assumed to be a reasonable approximation. Figure 2 shows a time series of measured velocity component along the 20° direction at Station 2, together with the best statistical and Grønskei's prediction midway between Stations 3 and 4.

Although there was changing weather during the measurement period, data are few and the variability so small that all simultaneous observations of the two-dimensional wind field are assumed to be realizations from the same distribution.

2.2 Second order structure

Although utilization of time persistence could be formally simply taken into account by letting p and t in Equations (A6) of Appendix A span actual and previous times, this is not done here. Only the spatial structure is discussed.

Preliminar calculations indicated that the covariance matrices tend to be oriented along the 20° direction. A righthanded cartesian coordinate system, with the 2-axis along 20°, is therefore chosen. In this system the estimated mean wind and covariances are shown

in Tables 1 and 2. The mean wind is small at all stations. The principal axis of any covariance matrix does not vary more than $\pm 10^{o}$ from the 2-axis in the chosen system. Each wind component in this system may therefore be treated as a scalar (compare Equation A6).

The covariance estimates in Table 2 appear to be influenced by local and stochastic variations. Little or no systematic and significant variation with distance is revealed. In this situation the choice of covariance function must be subjective and simple. A homogeneous field, with exponential autocovariance of integral scale comparable to the terrain features for the area, ($I \simeq 20$ km), is chosen for both independent velocity components. The same line of argument suggests that the relative measurement error, appearing in $Q^{*}_{ij}(p,q)$ of Equation (A4) be subjectively chosen (probably too small) as $10^{-2}\delta_{ij}\delta_{pq}$. As a consequence of this, and what is said about poor conditioning in Appendix A2, the statistical predictions should then be considered as objectively "reasonable" only.

2.3 Prediction error as function of the measurement network

Figure 3 shows the theoretical minimum error field for the chosen correlation function in the case where all 5 measurement stations are used for prediction. In the neighbourhood of one station and far away from all, the prediction accuracy is little affected by the presence of more than one station. Removing or adding stations gives results that resemble simple extrapolations based on Figure 3. A main message is that if accurate prediction at <u>one</u> location is desired, nothing is as efficient as a measurement there. A more detailed discussion of theoretical prediction errors is given by Eidsvik (1978).

Figure 4 illustrates the estimated mean and covariance matrices for the error field $[u_i(\underline{x}_p) - \hat{u}_i(\underline{x}_p)]$ at the Stations 6 and 7. In the error computations, a station is assigned to the nearest grid point of a grid with 1 km resolution. While the error is reasonably small and isotropic at Station 6, it is large and anisotropic at Station 7. The main axis of the latter is oriented

along the fjord. The figure suggests that statistical prediction based upon 5 stations in Oslo can not even predict, with useful accuracy, whether the flow is in or out of the fjord. While it could probably be easy to agree on what were large or small errors in the latter cases, this will not generally be so. For the purpose of this study we will subjectively consider ca 1 ms^{-1} as an approximative border between accurate and inaccurate predictions.

To facilitate the discussion of vectorial error at one location, the determinant of the error covariance matrice is introduced as a quality measure (compare Akaike, 1971). If we prefer to think in terms of "typical standard deviation", it is the 4th root of this determinant. Figure 5 shows the theoretical and estimated determinants. The similarity between the two is excellent at Stations 6 and 4. This indicates that the theoretical error field is realistic over the area "spanned by" the measurement stations. The theoretical determinant is obtained as $\{E^*\varepsilon_j^2\}\overline{|Q_{ij}(p,p)|^p}$. Here $E^*\varepsilon_i^2$ is the normalized error, computed analogously to those in Figure 3, and $\overline{|Q_{ij}(p,p)|^p} \simeq 8.3\ (ms^{-1})^4$ is the mean value of the determinants obtained as the product of the canonical variances in Table 2.

A representative error for the field between the Stations 1, 2, 3 and 4 is, as indicated in Figure 3, $E^*\varepsilon_i^2 \simeq 7 \cdot 10^{-2}$, leading to a typical theoretical standard deviation there of ca 0.5 ms^{-1}, as compared to the total $(\overline{|Q_{ij}(p,p)|^p})^{1/4} \simeq 1.7\ ms^{-1}$. Associated with the latter accuracy is no cost, while with the former are the high operation cost of 4-5 measurement stations. This indicates that accurate wind field prediction may be expensive.

3 COMPARISON WITH GRØNSKEI'S PHYSICAL PREDICTION MODEL

The estimates at Station 7 in Figure 4 suggest that increased accuracy could be obtained if the physics of the wind field were utilized for prediction. Grønskei's (1973) model, outlined in Appendix B, is "physical" but it also uses the data from Station 7

as input, so that its data cannot be used for verification. His other input stations were: Nydalen (1), Valle Hovin (2) and Husebye (8), (Grønskei et al. 1973). Grønskei's stations have data from 1 December 1970 to 13 January 1971 only.

3.1 Wind components

The errors obtained by Grønskei's prediction, illustrated in Table 3 and 4 are comparable to those obtained by the statistical model. The error at Station 5 indicates that physical models may also be inaccurate when the prediction location is too far away from the input stations. The estimated spatial correlation of the error field may be significant.

It now remains to compare the two estimates. As indicated in Figure 2, the time developments of the larger scales are reasonably well modelled by both methods. As indicated by Figure 6, the largest mean difference is located in the neighbourhood of stations used by only one of the prediction methods. Since the mean velocity difference is reasonably small over the most interesting parts of the field, the determinant of the mean quadratic velocity difference is a reasonable measure for the similarity. Figure 7, when compared with Figures 5 and 3, shows good similarity between the two prediction methods in the area spanned by the common measurement stations 1 and 2. Here it is interesting that the statistical method, which contains no explicit terrain effects, predicts much the same wind as the physical model, designed to take terrain explicitely into account. Over the central part of Oslo, where the pollutant sources are, the difference between the two predictions is comparable to the deviation between two independent flow estimates each with an error of ca 0.5 ms^{-1}, that is; almost 1 ms^{-1}. The disagreement is large near Station 5, which was not used in Grønskei's prediction, and near Station 7, which is not used in the statistical prediction. It is particularly large near Station 7 where the wind variations were much larger than at the other stations.

3.2 Divergence

A main feature of Grønskei's model is that the horizontal convergence is assumed proportional to the heat production. The wind data are only used for estimating the nondivergent part of the flow. The statistical model has no such assumption. It turns out that the objectively estimated divergence has largest magnitude in the area spanned by the measurement stations and becomes very small outside this area. Since the measurement stations are located in the (warm) town, this could be a physically beautiful result. However, since the optimally predicted wind field must approach a constant far away from the measurement stations, it is a methodological necessity and therefore a physically inconclusive result. The discussion is therefore restricted to a location where both methods are expected to be reasonably accurate, midway between Stations 3 and 4. Velocity derivatives are estimated over finite distances of 4 km. The estimated mean and standard deviation of the divergence estimate for the statistical model are $-1.4 \cdot 10^{-4} s^{-1}$ and $2.4 \cdot 10^{-4} s^{-1}$, respectively, and $-6.6 \cdot 10^{-4} s^{-1}$ and $2.1 \cdot 10^{-4} s^{-1}$, respectively, for the Grønskei model. The correlation between the two estimates turns out to be insignificant. Since divergence estimates must be inaccurate, the two estimates are judged to be surprisingly similar. The objective estimate of negative horizontal divergence suggests that the heat island effect (Grønskei, 1973) in the Oslo winter flow is real.

4 CONCLUDING REMARKS

Although the statistical prediction applied must be considered as highly idealized as compared to the complicated Oslo wind field, the theoretical error variance agrees well with the actual in the area "spanned by" the measurement locations.

Within this area, Grønskei's physical model is estimated to predict the wind field with approximately the same accuracy as the statistical model, ca 0.5 ms^{-1}.

Outside this area, and/or in areas where field inhomogeneities are too pronounced, both models may have larger errors than the esti-

mated total variability (ca 1.7 ms^{-1}) so that they are useless for predictions there.

In the area spanned by common measurement stations, the statistical model predicts approximately the same flow as the physical model, even if it takes no explicite account of the terrain. Terrain effects are probably implicite in the data.

The characteristic minimum prediction error of ca 0.5 ms^{-1} is associated with the characteristic total variation of ca 1.7 ms^{-1}. In other flows, the minimum prediction error would probably vary approximately linearly with the characteristic total variability.

It appears that many measurement stations, located so that they span the area of interest, are neccesary for accurate wind field estimation. With such data, it could be that the prediction method must be very sophisticated if it shall be significantly more accurate than simple ones.

ACKNOWLEDGEMENTS

The author is indebted to Sam-Erik Walker who solved the systems of equations (A6) on the computer and to Knut Erik Grønskei who provided the data and winds from his physical flow model. The present computations were done by Kurt Østgård.

5 REFERENCES

Akaike H. 1971: Autoregressive model fitting for control. *Ann.Inst.Statist.Math.* 23, 163-180.

Eidsvik K.J. 1978: On near optimal interpolation and extrapolation of atmospheric variables using a few measurement stations. Technical Note VM-295. Norwegian Defence Research Establishment, Kjeller.

Eidsvik K.J. 1980: A surveillance system for air pollutions. NILU TN NR 6/80. (In Norwegian.)

Eidsvik K.J. 1981: On the prediction of hazard area resulting from a gas release. NILU OR NR 1/81. Lillestrøm.

Gandin L. 1965: *Objective analysis of meteorological fields.* Hydrometeor, Publ. House, Leningrad. Translation Jerusalem, p 242.

Goodin W.R., Gregory J., Mc Rae and Seinfeld J.H. 1980: An objective analysis technique for constructing three-dimensional urban-scale wind fields. *Appl. Meteorol.*, 19, 98-108.

Granger C.W.J. 1975: Aspects of the analysis and interpretation of temporal and spatial data. *The Statistican*, 24, p 197-210.

Grønskei K.E., Joranger E., Gram F. 1973: Assessment of air quality in Oslo, Norway. Appendix D in: *Guidelines to assessment of air quality (Revised)* SO_4, *TSP, CO, HC,* NO_x *and oxidants.* NATO/CCMS, nr. 6.

Grønskei K.E. 1973: Comparison between a physical dispersion model and a statistical model for ambient SO_2-concentration in Oslo. In: *Proceedings of the third International clean air congress.* Düsseldorf, Federal Republic of Germany. B3.

Katayama T. 1980: Estimation of images modelled by a two-dimensional separable autoregressive process. *IEEE. Trans on Automatic Control.* AC-25, 1199 - 1201.

Olea R.A. 1975: Optimum mapping techniques using regionalized variable theory. *Series on Spatial Analysis, no 2,* Kansas Geological Survey, p 137.

Sasaki Y. 1970: Some basic formalisms in numerical variational analysis. *Monthly Weather Review,* 98, p 875-883.

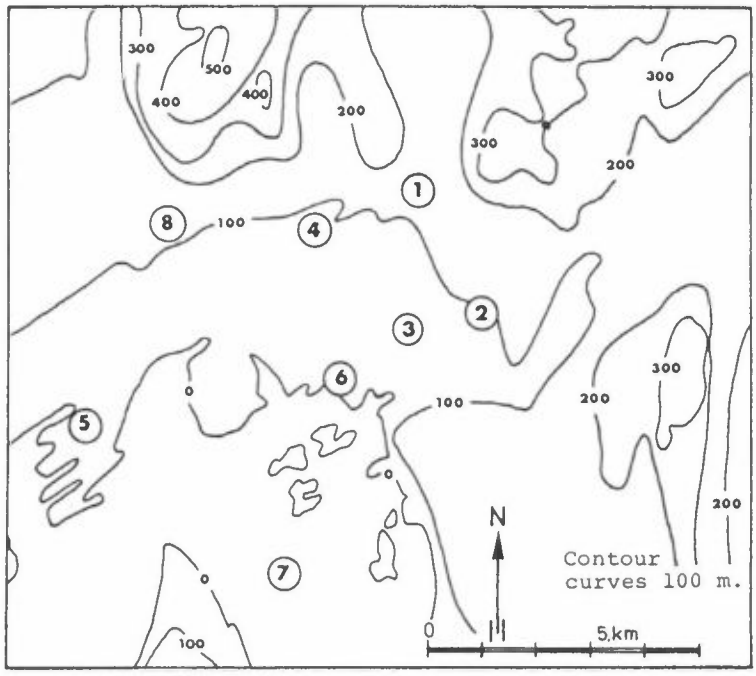

Figure 1: Wind measurement stations in the Oslo area. 1: Nydalen. 2: Valle Hovin. 3: Munchmuseet. 4: Meteorological Institute, Blindern. 5: Fornebu Airport. The stations 6: Vika, 7: Husebergøya and 8: Huseby have less and poorer quality data.

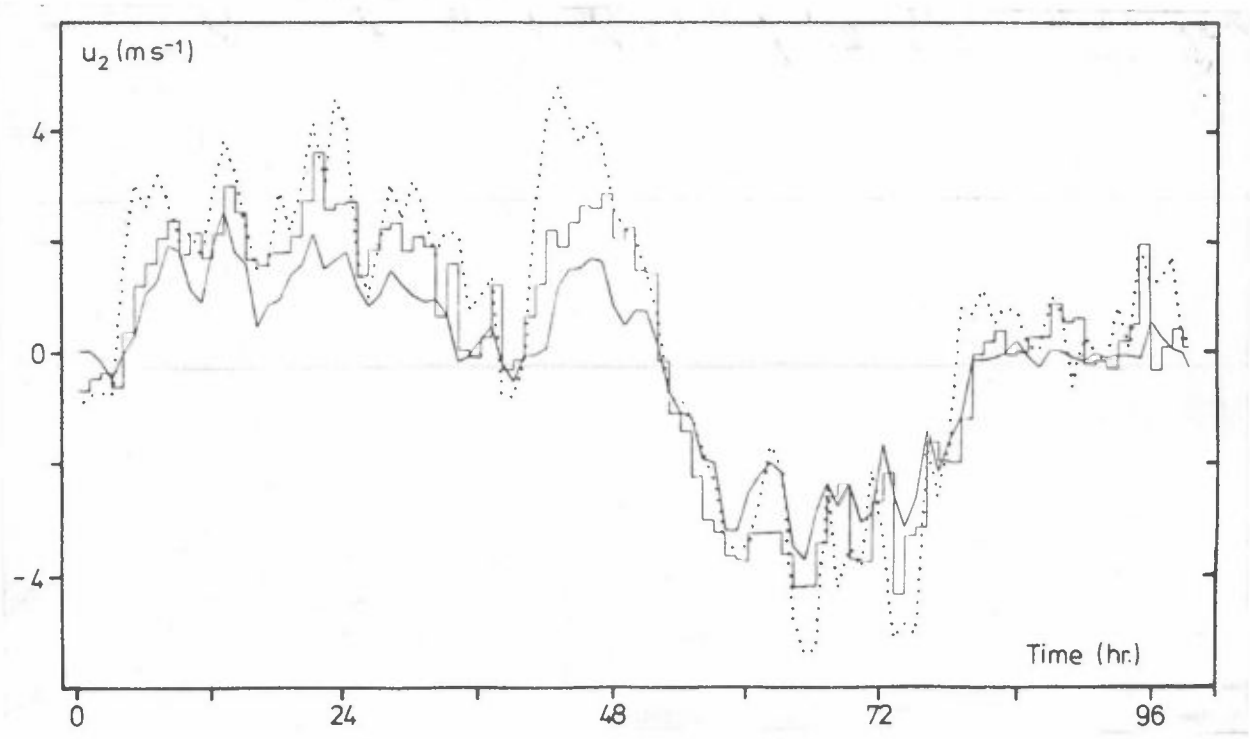

Figure 2: Actual hourly wind components along 20° at Station 2 and predicted values at a location midway between Station 3 and 4. ..... Actual. _┌ Grønskei's. ∧ statistical. This interval contains the largest wind variations during the measurement period.

Table 1: Estimated mean horizontal wind at the five stations. A righthanded cartesian coordinate system with 2-axis along 20° is used. Unit (ms^{-1}).

i \ p	1	2	3	4	5
1	-.3	-.6	-.4	-.1	-.0
2	-.6	-.2	-.1	-.3	-.2

Table 2: Estimated covariance matrices of horizontal wind for different components and locations. A righthanded cartesian coordinate system with 2-axis along 20° is used. Also in canonical form with the principal axis direction in degrees. Units: m and s.

p	q	$\lvert \underline{x}_p - \underline{x}_q \rvert \cdot 10^{-3}$	$Q_{ij}(p,q)$			Canonical form		
			11	12	22	2'2'	1'1'	ϕ
1	1	0.0	1.3	-.3	6.1	6.1	1.2	-86
2	2	0.0	1.5	.0	6.4	6.4	1.5	90
3	3	0.0	.7	.2	2.2	2.3	.7	81
4	4	0.0	.5	-.2	1.8	1.8	.4	-81
5	5	0.0	1.9	-.2	4.4	4.4	1.9	-85
2	3	1.7	.7	-.1	3.5	3.5	.7	-88
3	2	1.7	.7	-.6	3.5	3.6	.6	79
1	4	2.5	.5	-.2	2.9	2.9	.5	-86
4	1	2.5	.5	-.4	2.9	3.0	.5	-81
1	3	3.4	.5	-.2	3.2	3.2	.5	-86
3	1	3.4	.5	.4	3.2	3.3	.4	82
1	2	3.9	.9	-.3	5.5	5.5	.9	-87
2	1	3.9	.9	-.0	5.5	5.5	.9	-90
3	4	4.4	.2	.2	1.7	1.7	.2	83
4	3	4.2	.2	-.3	1.7	1.7	.2	-80
2	4	5.5	.5	-.0	2.8	2.8	.5	-90
4	2	5.5	.5	-.4	2.8	2.9	.5	-81
4	5	8.0	.7	-.3	2.2	2.2	.6	-79
5	4	8.0	.7	-.3	2.2	2.2	.6	-80
3	5	9.6	.6	.2	2.5	2.5	.5	83
5	3	9.6	.6	-.3	2.5	2.5	.5	-81
1	5	10.3	1.0	-.2	4.1	4.1	1.0	-87
5	1	10.3	1.0	-.5	4.1	4.1	.9	-82
2	5	11.3	1.0	-.2	4.2	4.2	1.0	-86
5	2	11.3	1.0	-.5	4.2	4.2	1.0	-82

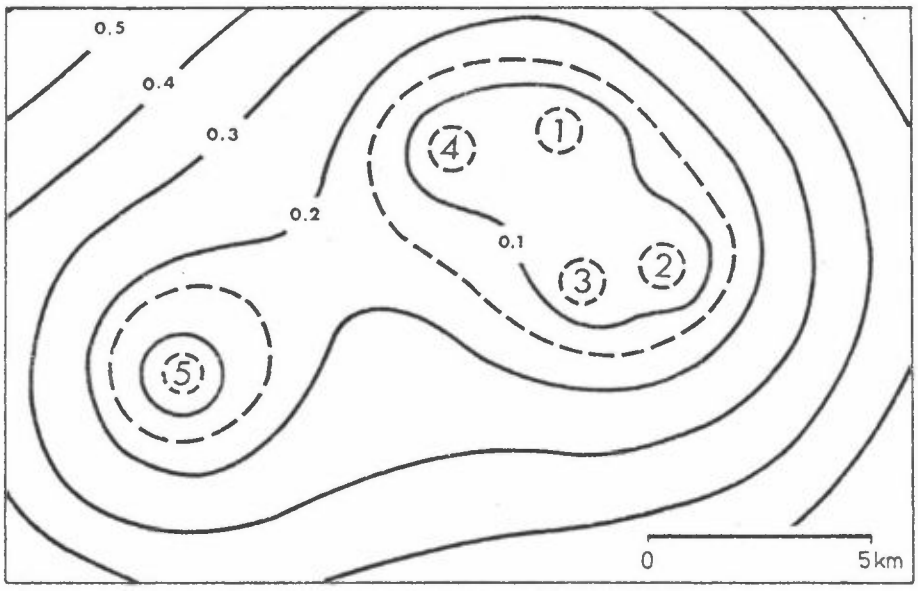

Figure 3: Theoretical minimal prediction variance relative to unit variance, with the 5 stations of Figure 1 used for prediction.

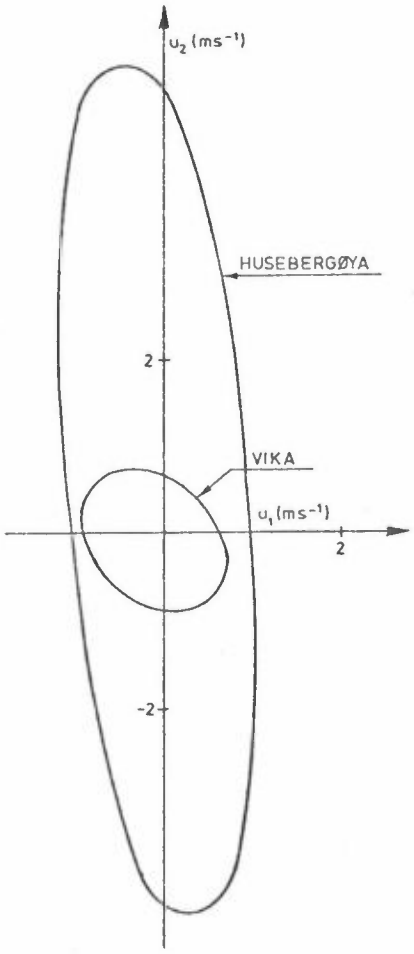

Figure 4: Estimated minimal error at Vika (6) and Husebergøya (7), with the 5 stations of Figure 1 used for prediction. Standard deviation ellipsoide superimposed on mean value . (N = 697). Righthanded cartesian coordinate system with u_1 along East.

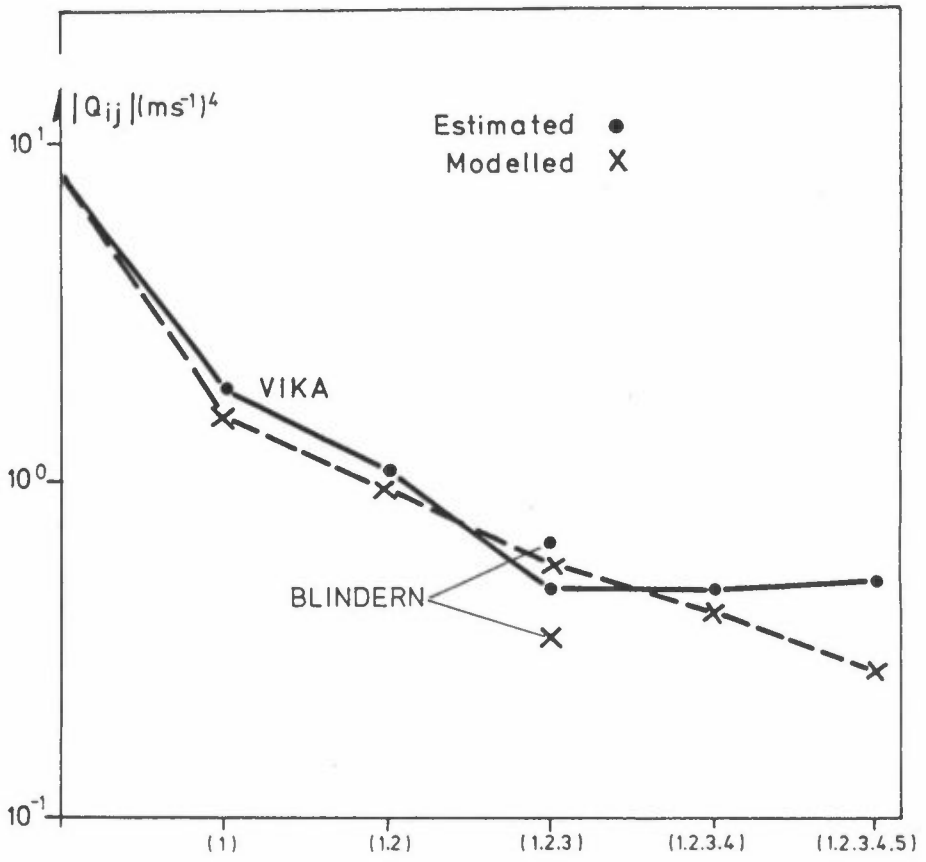

Figure 5: Estimated minimum error covariance determinant at Vika as varying with the measurement network parametrized as in Figure 1. (N = 697) and at Blindern, (N = 2160).

Table 3: Estimated mean difference between Grønskei's prediction and actual. North-East cartesion coordinate system. Unit: (ms^{-1}).

p / i	5	4	3
1	.1	.3	-.2
2	-.3	-.5	.5

Table 4: Estimated error covariance for Grønskei's wind model. North-East cartesian coordinate system. Also in canonical form with principal axis direction in degrees. Units: m and s.

p	q	$\lvert \underline{x}_p - \underline{x}_q \rvert \cdot 10^{-3}$	$Q_{ij}(p,q)$			Canonical form		
			11	12	22	2'2'	1'1'	ϕ
5	5	0.0	2.6	.9	1.9	3.2	1.2	34
4	4	0.0	.6	.2	.6	.8	.4	44
3	3	0.0	.5	-.1	.9	.9	.5	-77
4	3	4.2	.2	.2	.5	.6	.0	61
3	4	4.2	.2	-.0	.5	.5	.2	-81
5	4	8.0	.6	-.1	.4	.6	.3	-20
4	5	8.0	.6	.2	.4	.7	.2	33
5	3	9.6	.3	-.2	.3	.5	.1	-44
3	5	9.6	.3	.3	.3	.6	.0	45

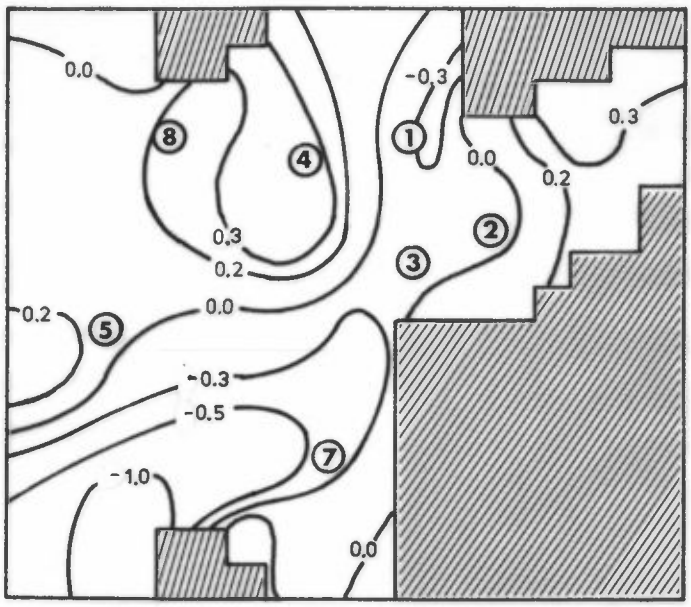

Figure 6a: Mean difference between the Grønskei and the statistical easterly wind component. Hatched areas represents mountains.

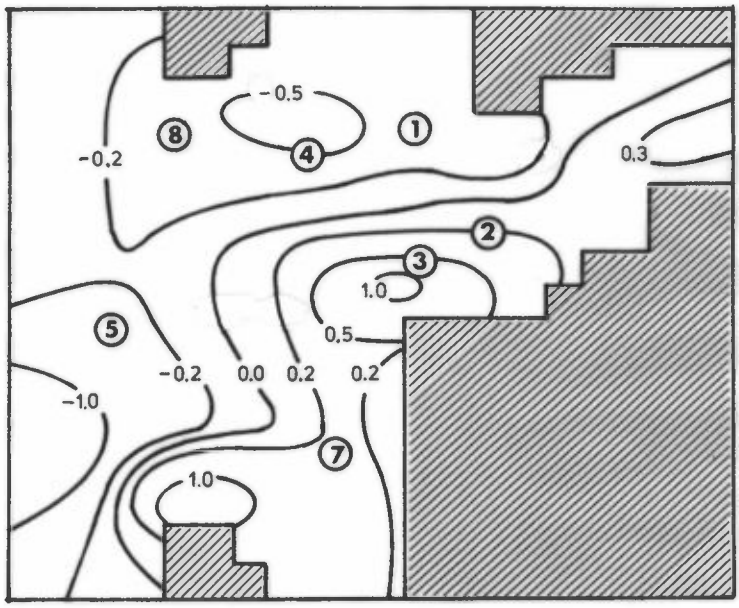

Figure 6b: Mean difference between the Grønskei and the statistical northerly wind component.

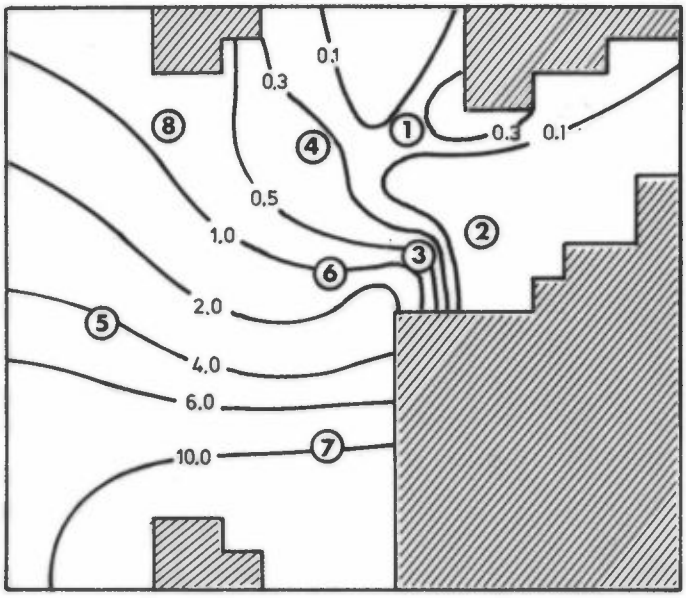

Figure 7: Isocurves for the determinant of the mean quadratic difference of the statistical and Grønskei's prediction. Hatched areas represents mountains.

APPENDIX A

A1 Optimal prediction of vectorial fields

Assume that the d-dimensional vector $\underline{u}$ is a stochastic field in S-dimensional space $\underline{x}$, possibly including time. $\underline{u}$ is measured at the n locations $\underline{x}_p$, p = 1...n, with additive, unbiased combined effect from small scale variations and measurement error $\underline{\varepsilon}(\underline{x}_p)$. Our problem is to find the "best" linear predictor (estimator) at the location $\underline{x}_o$

$$\hat{\underline{u}}(\underline{x}_o) = \sum_{p=1}^{n} \underline{\Phi}(\underline{x}_o, \underline{x}_p)[\underline{u}(\underline{x}_p) + \underline{\varepsilon}(\underline{x}_p)] \quad , \tag{A1}$$

with the dxd constraints

$$\sum_{p=1}^{n} \underline{\phi}(\underline{x}_o, \underline{x}_p) = I \quad . \tag{A2}$$

The constraints (A2) also make (A1) an unbiased estimator for a constant expected field. In component form, with summation convention used, the local prediction error at $\underline{x}_o$ is

$$\begin{aligned} R_i(\underline{x}_o) &= u_i(\underline{x}_o) - \hat{u}_i(\underline{x}_o) \\ &= - \Phi_{ij}(\underline{x}_o, \underline{x}_p)[u_j(\underline{x}_p) + \varepsilon_j(\underline{x}_p)] \\ &= - \phi_{ij}(p)[u_j(p) + \varepsilon_j(p)]. \end{aligned} \tag{A3}$$

Here the location in S-dimensional space is indexed with p only, and the summation extended from p=0 with the understanding that $\Phi_{ij}(0) = -\delta_{ij}$ and $\varepsilon_j(0) = 0$. When $Q^*_{jk}(p) = E[u'_j(p) + \varepsilon_j(p)]$ $[u'_k(q) + \varepsilon_k(q)]$, the expected prediction error is

$$ER_i^2(\underline{x}_o) = \Phi_{ij}(p)\ \Phi_{ik}(q)\ Q^*_{jk}(p,q) \quad . \tag{A4}$$

Introducing the Lagrange multipliers μ_{ij}, the best prediction conditional to Equation (A2) is found by minimizing the expression

$$ER_i^2 + 2\mu_{ij}[\sum_{p=1}^{n} \Phi_{ij}(p) - \delta_{ij}]. \qquad (A5)$$

Equating the differensiations with respect to $\Phi_{rs}(t)$, $(r,s,t) > 0$ to zero, gives the condition

$$\sum_{p=1}^{n}\sum_{j=1}^{d} \Phi_{rj}(p)\, Q^*_{js}(p,t) + \mu_{rs} = Q^*_{rs}(o,t)$$

$$\sum_{p=1}^{n} \Phi_{rs}(p) = \delta_{rs} \quad . \qquad (A6)$$

These dxdxn+dxd linear equations determine the unknown $\Phi_{rs}(p)$ and μ_{rs}. Fortunately, they are separable in r so that it suffices to solve dxn+d linear equation for each r. If a coordinate system can be found such that $\Phi^*_{js}(p,t) \propto \delta_{js}$ for all (p,t), the equations are also separable in s so that the problem reduces to the usual one of solving n+1 equations for each (scalar) variable u_i. This simplification is probably sometimes accurate enough also when decomposition of the vector into a curvelinear system is necessary to achieve this, without other explicite modifications for coordinate transformations. The minimum prediction error is given when $\Phi_{ij}(p)$, as obtained from Equation (A6), is introduced into Equation (A4).

Equations (A6) and (A4) may also be expressed in terms of the structure function $D_{ij}(\underline{x}_p,\underline{x}_q) = E[u_i(\underline{x}_p)-u_i(\underline{x}_q)][u_j(\underline{x}_p)-u_j(\underline{x}_q)]$, allowing discussion of fields with nondefined $Q_{ij}(\underline{x}_p,\underline{x}_p)$. Assuming white measurement error, $E\varepsilon_i(\underline{x}_p)\varepsilon_j(\underline{x}_q) = \delta_{ij}\delta_{pq}E\varepsilon_i^2(\underline{x}_p)$, the equation corresponding to Equation (A6) would then read

$$\sum_{j=1}^{d}\sum_{p=1}^{n} \Phi_{rj}(p)[D_{rs}(p,t) - 2\delta_{js}\delta_{pt}E\varepsilon_j^2(p)] + \mu^*_{rs} = D_{rs}(o,t)$$

$$\sum_{p=1}^{n} \Phi_{rs}(p) = \delta_{rs} \quad . \qquad (A7)$$

Since $D_{rs}(p,t)$ is minimal and $Q_{rs}(p,t)$ maximal along the diagonal, the system (A7) is not diagonally dominated like (A6). This favour the use of Equation (A6) for numerical solutions. However, a "general" solution procedure would formally handle them both, just by changing the input.

Provided that the second order structure of $\underline{u}(\underline{x})$ is estimated, which may be difficult, the Gandin prediction problem is thus formally simple, also for nonhomongeneous vectorial fields.

A2 Poor conditioning

The Equation (A6) (or A7) is in principle of the form $\underline{A}\underline{y} = \underline{b}$, where the matrix $\underline{A}$ and vector $\underline{b}$ are associated with $Q_{ij}(p,q)$ and the vecor y with $\Phi_{ij}(p)$. Textbooks on matrix theory give the relative uncertainty in y as a function of the assumed small uncertainty in $\underline{A}$ and $\underline{b}$ as

$$\frac{||\delta\underline{y}||}{||\underline{y}||} \leq \frac{\gamma}{1-\gamma\dfrac{||\delta\underline{A}||}{||\underline{A}||}} \left\{ \frac{||\delta\underline{A}||}{||\underline{A}||} + \frac{||\delta\underline{b}||}{||\underline{b}||} \right\} \quad . \tag{A8}$$

Here $||y||$ is a vector norm and $||\underline{A}||$ the related matrix norm. The condition number

$$\gamma = ||\underline{A}^{-1}|| \cdot ||\underline{A}|| \geq e_1/e_n \geq 1 \quad , \tag{A9}$$

is a measure of the conditioning of the equations. Here e_1 and e_n are the largest and smallest eigenvalues of $\underline{A}$ respectively. As seen from Equation (A8), the solution is well conditioned when γ is small. The condition number is computed for a homogeneous scalar field with exponential correlation function of integral scale I, 4 equally spaced stations with measurement error $E\varepsilon^2$ are located on a circle of radius R. The very large condition number, especially in the area of accurate prediction, is illustrated in Figure A1. This means that uncertainties on the second order

structure of $\underline{u}(\underline{x})$ results in large variations in the optimal prediction scheme, $\Phi_{ij}(p)$. However, the prediction accuracy need not vary much with varying method. Any "reasonable" prediction method may be nearly optimal (Eidsvik, 1978).

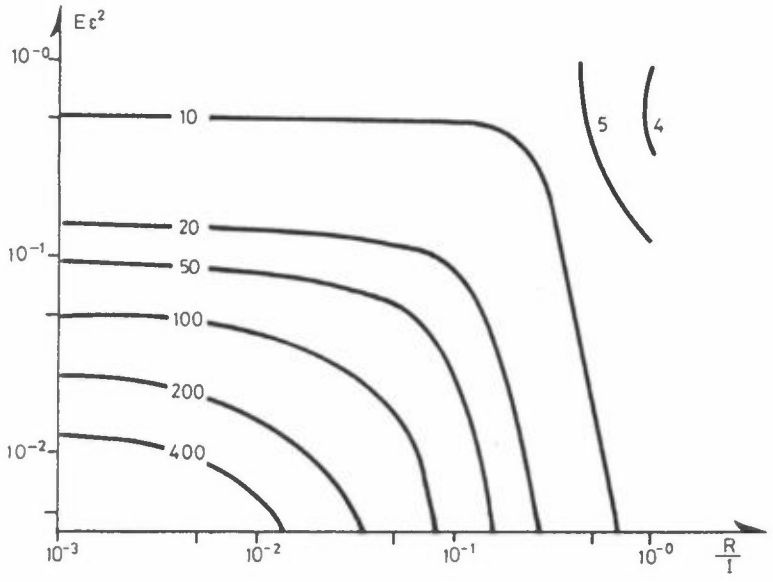

Figure A1: Isocurves for the condition number (largest eigenvalue divided by smallest). Four equally spaced stations on a circle of radius R.

APPENDIX B

A model for locally dominated flows over Oslo (Grønskei 1973):

The velocity potential χ, is based on height integration of the continuity equation and the thermodynamic energy equation, suggesting that the vertical velocity is proportional to the heat production. Over the city this is assumed to be proportional to the SO_2 release and over the fjord proportional to the tempreature difference between the air and water.

$$\nabla_2^2 \chi = \begin{cases} \alpha_1 \dfrac{dQ_{SO_2}}{dt} & \text{over the city} \\ \alpha_2 (T_a - T_w) & \text{over the fjord} \end{cases} \qquad \text{(B1)}$$

Here α_1 and α_2 are experimental coefficients. Boundary conditions are chosen as $\chi = 0$ to minimize the kinetic energy of the divergent wind.

The stream function ψ, is based on setting the vorticity equal to zero

$$\nabla_2^2 \psi = 0. \qquad \text{(B2)}$$

Boundary conditions are chosen as follows: The terrain is modelled as impermeable hatched areas in the Figures 6 and 7. Along the lower open boundary the flux is estimated using the u_2-component of Station 7 (corrected for the divergent wind). Along the right hand open boundary the flux is estimated using the u_1-component of Station 2. Along the upper bounded, open boundary the flux is estimated using the u_2-component of Station 1. Along the upper left open corner the flux is estimated using the u_1- and u_2-components of Station 8. Along the lower left open corner the flux is estimated so that the mass in the whole area be conserved.

NORSK INSTITUTT FOR LUFTFORSKNING
(NORGES TEKNISK-NATURVITENSKAPELIGE FORSKNINGSRÅD)
POSTBOKS 130, 2001 LILLESTRØM
ELVEGT. 52.
TLF. (02) 71 41 70

RAPPORTTYPE	RAPPORTNR.	ISBN--82-7247- 244-9
TEKNISK NOTAT	TN 6/81	
DATO	ANSV.SIGN.	ANT.SIDER
MAI 1981	B. Ottar	23

TITTEL
Estimering av horisontalt vindfelt over Oslo basert på få målestasjoner

PROSJEKTLEDER
K.J. Eidsvik

NILU PROSJEKT NR
01080

FORFATTER(E)
Karl J. Eidsvik

TILGJENGELIGHET **
A

OPPDRAGSGIVERS REF.

OPPDRAGSGIVER
NTNF

3 STIKKORD (á maks.20 anslag)
Vindfelt | Estimering | Feil

REFERAT (maks. 300 anslag, 5-10 linjer)

Romlig egenskaper ved vindfeltet over Oslo er analysert ved hjelp av data fra 8 målestasjoner. En homogen og isotrop versjon av Gandins teori for optimal interpolasjon ser ut til å estimere varslingsfeil med bra nøyaktighet.

TITLE

ABSTRACT (max. 300 characters, 5-10 lines)

**Kategorier: Åpen - kan bestilles fra NILU A
Må bestilles gjennom oppdragsgiver B
Kan ikke utleveres C